The European Zoological Journal

ISSN: 2475-0263 (Online) Journal homepage: www.tandfonline.com/journals/tizo21

A microscopical and ultrastructural analysis of the embryonic epidermis of the pool frog, *Pelophylax lessonae* (Camerano, 1882) (Anura: Ranidae)

D. SEMERARO, D. MENTINO, R. ROSSI, G. SCILLITANI, M. V. GUGLIELMI & M. MASTRODONATO

To cite this article: D. SEMERARO, D. MENTINO, R. ROSSI, G. SCILLITANI, M. V. GUGLIELMI & M. MASTRODONATO (2024) A microscopical and ultrastructural analysis of the embryonic epidermis of the pool frog, *Pelophylax lessonae* (Camerano, 1882) (Anura: Ranidae), The European Zoological Journal, 91:2, 1167-1177, DOI: 10.1080/24750263.2024.2422089

To link to this article: https://doi.org/10.1080/24750263.2024.2422089

Published online: 14 Nov 2024.

The European Zoological Journal, 2024, 1167–1177
Vol. 91, No. 2, https://doi.org/10.1080/24750263.2024.2422089

A microscopical and ultrastructural analysis of the embryonic epidermis of the pool frog, *Pelophylax lessonae* (Camerano, 1882) (Anura: Ranidae)

D. SEMERARO [1,a], D. MENTINO [2,a], R. ROSSI [2], G. SCILLITANI [1,3]*, M. V. GUGLIELMI [3,b], & M. MASTRODONATO [1,b]

[1]*Department of Biosciences, Biotechnology and Environment, University of Bari Aldo Moro, Bari, Italy,* [2]*Department of Precision and Regenerative Medicine and Ionian Area, University of Bari Aldo Moro, Bari, Italy, and* [3]*Institute for Water Research (IRSA), National Research Council (CNR), Taranto, Italy*

(Received 21 May 2024; accepted 13 October 2024)

Abstract

We analysed the embryonic epidermis of the pool frog, *Pelophylax lessonae*, by light and electron microscopy techniques, and characterized preliminarily its mucous secretions with conventional histochemistry (Toluidine Blue, Periodic Acid-Schiff, Alcian blue pH 2.5 and Alcian blue pH 1.0). At Gosner's developmental stage 21, the epidermis consisted of a bilayered epithelium with five cell types. Basal cells (BCs) constituted the basal layer, presented a large nucleus and were sometimes observed in mitosis. Ciliated cells (CCs) had a ciliated apical membrane, with carboxylated glycans in the sub-apical portion. TEM analysis revealed small vesicles just below the surface, a central nucleus, and evident yolk plates. Goblet cells (GCs) and small secretory cells (SSCs) showed secreting vesicles and vacuoles, respectively. In the mucus secretion of GCs sialosulphomucins appeared, while in that of SSCs sulphation was not observed. Under TEM, GCs had irregular shaped nuclei and a less electron-dense cytoplasm with respect to SSCs. Ionocytes (INs) presented apical microvilli and a high electron-dense cytoplasm with vacuoles. SEM analysis revealed that GCs outnumbered the other cell types and that SSCs and INs were usually located together near to GCs. The relatively simple structure of the epidermis and its direct interfacing with the environment renders it a good model for the study of structure and development of mucociliary epithelia, as well as of its alterations in the presence of toxicants.

Highlights

- The embryonic epidermis of *Pelophylax lessonae* reveals a good model for the study of mucociliary epithelia.
- The embryonic epidermis of *Pelophylax lessonae* is made of two layers and five cell types.
- In the basal layer, there are basal cells, and in the apical layer, ciliated, goblet, and small secretory cells are found, as well as ionocytes.
- Goblet cells present secreting vesicles with sialosulphomucins. Small secretory cells show apical vacuoles with sialomucins only.

Keywords: Pelophylax lessonae, *embryology*, *mucociliary epidermis*, *histochemistry*, *ultrastructure*

Introduction

The skin of amphibians has been long regarded as a model to study the regulation of water and solute movements across membranes due to its relative permeability (Helmer & Whiteside 2005; Burggren & Warburton 2007; Quaranta et al. 2009). Besides, the life cycle of many species, with an aquatic larva evolving into a terrestrial adult through a complex metamorphosis, focused research on the deep

*Correspondence: G. Scillitani, Department of Biosciences, Biotechnology and Environment, University of Bari Aldo Moro Via Orabona 4, Bari 70125, Italy. Email: giovanni.scillitani@uniba.it
[a]Joint first authors.
[b]Joint senior authors.

changes their skin undergoes (Duellmann & Trueb 1986; Akat Çömden et al. 2023). Also, the embryonic development of the integument is studied by morphological and genetic approaches to understand the differentiation processes and their modulation (e.g., Billett & Gould 1971; Brändli 2004). Both the ciliogenesis and the secretion of embryonic epidermis are regarded as models in studies about the mucociliary epithelia, such as those covering the inner surfaces of the human upper respiratory system (although of different embryologic origin: e.g., Dubaissi & Papalopulu 2011; Walentek & Quigley 2017; Sim et al. 2018). Being the direct interface with environment, the skin is one of the organs more susceptible to toxicants and to infection diseases (Quaranta et al. 2009; McCoy & Peralta 2018; Varga et al. 2019). Thus, it has become a model in ecotoxicological studies (e.g., Allran & Karasov 2001; He et al. 2014; Johnson et al. 2017; Do Amaral et al. 2019).

Most studies were performed on the well-known amphibian models of the genus *Xenopus* (Fox & Hamilton 1971; Harland & Grainger 2011; El Mir et al. 2023), but data are also available on embryos and larvae of anurans from both the New and the Old World (e.g., Leeson & Threadgold 1961; Fox 1974; Rosenberg & Warburg 1978; Robinson & Heintzelman 1987; Fenoglio et al. 2006; Delfino et al. 2007; Giachi et al. 2011; Chammas et al. 2015). The cited papers underline that many cell types in the skin develop in a relatively short time and then degenerate or evolve into other cell types (Robinson & Heintzelman 1987). It is difficult to compare the results from different papers, since many authors did not uniform the cell nomenclature used by others, and few attempted a comparison through literature. In general, six main types of cells can be observed (Duellmann & Trueb 1986; Fox 1986; Giachi et al. 2011).

Basal cells are relatively undifferentiated cells forming the inner layer of epidermis. They are involved in proliferation and differentiation of the other cell types (Billett & Gould 1971; Nishikawa et al. 1990).

Goblet or mucous surface cells have an important physiological role in the production and storage of fluid and mucous materials (Akat Çömden et al. 2023). Secretion products are stored in the cell as granules and then released in response to external stimuli.

Small secretory cells (SSCs) have many electron-dense granules apically and are hypothesized to produce a mucous protective layer, which is likely moved away by the actions of the cilia of the ciliated cells (Hayes et al. 2007; Dubaissi et al. 2018), as well as serotonin, which functionally regulates ciliary beat frequency and speed of mucus transport (Walentek et al. 2014; Dubaissi et al. 2014).

Ciliated cells are among the most observed cells. They seem to develop towards the end of the embryonic development and disappear soon after hatching. They are widely distributed over the surface of early tailbud stages (Haslam et al. 2014). The cilia have a prominent role in removing microorganisms or particles from mucus-covered surfaces (Akat Çömden et al. 2023).

Mitochondria-rich cells are probably involved in ion transport and osmoregulation; thus, they are named ionocytes or proton-secreting cells (Dubaissi & Papalopulu 2011; Quigley et al. 2011; Werner & Mitchell 2012). Anyway, their function is largely unknown.

Clear, Skein or Klugenzellen (Fröhlich et al. 1978; Fox 1988; Giachi et al. 2011) have a relatively clear cytoplasm with peripheral bundles of tonofilaments of larval keratin (the so-called figures of Eberth), with mechanical properties (Delfino et al. 2007).

With all the previous as reference, we performed a microscopical and ultrastructural analysis of the skin of the pool frog *Pelophylax lessonae*, a widespread European species in the *Pelophylax* kl. *esculentus* species-complex, which proved good models in environmental and toxicological studies (e.g., Guex et al. 2001; Loumbourdis 2005; Fenoglio et al. 2006, 2009; Mastrodonato et al. 2009; Zhelev et al. 2013; Mentino et al. 2017; Şişman et al. 2021). Although a number of studies are available about skin structure and development in adult and late larval stages (e.g., Guardabassi et al. 1975; Masoni & Garcia-Romeu 1979; Fenoglio et al. 2009), little is known about the structure of the skin and the cell types in earlier stages. Thus, we performed a detailed morphological study with multiple approaches to give a reference for further studies.

Material and methods

Material

Embryos of the pool frog, *P. lessonae*, were sampled from an artificial tank in the Botanical Garden of the University of Bari Aldo Moro, designed to reproduce a Mediterranean pond with the vegetation typical to Apulia. The systematics of European water frogs in the genus *Pelophylax* (previously included in the genus *Rana*) is made difficult by hybridogenetic events between species (Dufresnes et al. 2024) and

scarce morphological differentiation, so genetic analyses are required to assign a population to a species and detect hybridization (Cuevas et al. 2022). The frog population in the tank descends from some individuals released by a laboratory technician from the former Department of Physiology of the University of Bari Aldo Moro (Signorile, pers. comm.). They were bought from a dealer from Arzano (Naples) who caught them around Castel Volturno (Caserta, Campania) (De Rosa, pers. comm.). Frogs from the same area were sold by the cited dealer to researchers in the former Department of Zoology of the University of Naples Federico II who analyzed their genetic composition and ascribed them to the "Southern Italian nonhybrid" cluster (Paolucci et al. 1987), currently regarded as a subspecies of *P. lessonae*, named *P. l. bergeri* (Canestrelli & Nascetti 2008; Speybroeck et al. 2020).

Experimental design

Embryos at the Gosner's developmental stage 11, i.e., earliest involution of blastopore dorsal lip (Gosner 1960), were randomly selected from three different clutches. The eggs were subsequently randomly divided into three Petri dishes with native water. Groups were kept in a thermostatic chamber at 18°C and light cycle of 12 h, corresponding about to the environmental conditions of the tank. After 10 days, most embryos were at Gosner's stage 21 (corresponding to gill and adhesive gland development and transparent cornea: Gosner 1960). Normally developed embryos were selected under a stereomicroscope at 2X and subjected to the morphological analysis. Since the study involved amphibian embryos, it does not remit within the terms of the Decree Law No 26 of 4 March 2014 (Implementation of the Directive 2010/63/EU on the protection of animals used for scientific purposes). Anyway, an opinion was asked to the Commission for Animal Welfare of the Department of Biology of the University of Bari Aldo Moro (in which the experiments took place) that expressed favourably (Commission for Animal Welfare of the Department of Biology of the University of Bari Aldo Moro, meeting minute 28.09.2022)

Light microscopy

For light microscopy embryos were embedded in Technovit 8100 (Heraeus Kulzer, Hanau, Germany) (Mentino et al. 2014). Six individuals were fixed in a 2% paraformaldehyde solution in 0.1 M phosphate-buffered saline (PBS), pH 7.4 at 4°C for 3 h, then washed in PBS and incubated overnight in PBS with sucrose 6.8% at 4°C. After dehydration in an increasing graded series of acetone (50−100%) at 4°C, they were transferred in a solution with 15:1 pre-cooled infiltrating solution overnight. Subsequently, samples were infiltrated in a polymerisation solution and then embedded in forms on a cooling plate of ice at 4°C to promote polymerisation (e.g., Mastrodonato et al. 2017). Semithin sections of the dorsolateral region of the embryos, 3 µm thick, were cut with glass knives using a PowerTome Ultramicrotomes (Boeckeler Instruments Inc., Tucson, AZ). Sections were mounted on microscope slides, coated with polylysine, permeabilized with 0.5% Trypsin in PBS, pH 7.5 for 30 min, at 37°C, and treated with 0,3% TritonX in PBS, at 37°C. For the examination of the general morphology, the sections were stained with Toluidine blue or Mallory's trichrome (e.g. Gristina et al. 2017).

Carbohydrates were characterised with Periodic-Acid Schiff (PAS), Alcian Blue pH 2.5 (AB 2.5), and Alcian Blue pH 1.0 (AB 1); each section was counterstained with Carazzi's hematoxylin. These stains detect the presence of general carbohydrates (PAS), acidic carboxylated and/or sulphated glycans (AB 2.5), and sulphated glycans (AB 1), respectively (e.g., Petraccioli et al. 2013). AB and PAS stain were combined to detect both acidic (stained blue-violet) and neutral (stained red) glycans according to Guglielmi et al. (2024). Otherwise specified, all the cited chemicals were from Merck-Sigma (Saint Louis, MO, USA).

Photos were captured using a light microscope Nikon Eclipse N*i* equipped with DS-Fi3 microscope-camera (Nikon Instruments Ltd, Campi Bisenzio, Florence, Italy).

Electron microscopy (SEM, TEM)

For scanning electron microscopy (SEM), six embryos were fixed in 2.5% buffered glutaraldehyde (TAAB Laboratories, England, UK), at 4°C for 4 h and then washed and incubated in PBS overnight. Samples were washed in distilled water and dehydrated in an ethanol series (from 70% to 100%) for 15 min at room temperature (RT) for each step. Critical point drying technique (Bray 2000) was performed before observation. Samples were glued onto aluminum stubs (Multilab type stub pin ½, Surrey, UK) using silver paste and coated with gold in a sputtering device (Edwards S150A Sputter Coater) and then observed at 15 kV with a Hitachi TM3000 scanning electron microscope (Hitachi Europe LLC, Ospiate di Bollate, Milan, Italy).

For transmission electron microscopy (TEM), six embryos were fixed in 2.5% buffered glutaraldehyde (TAAB Laboratories, England, UK), at 4°C for 4 h and then washed and incubated in PBS overnight. Specimens were post-fixed with 1% osmium tetroxide in PBS at 4°C for 2 h. After re-washing in the same buffer, specimens were dehydrated in a graded series of acetone and embedded in Epoxy Resin-Araldite (M) CY212 (TAAB Laboratories Equipment Ltd, Aldermaston, Berkshire, UK) (Tucci et al. 2016). Ultra-thin sections were mounted on Nickel grids and stained with uranyl acetate and lead citrate according to Scillitani et al. (2011).

Results

Light microscopy

The morphology of the embryos of *P. lessonae* at Gosner's stage 21 was observed with Mallory's trichrome. The dorsolateral region of the embryos was selected to analyse the epidermis (Figure 1). It consisted of two layers, a basal and an apical one (Figure 2(a,b)).

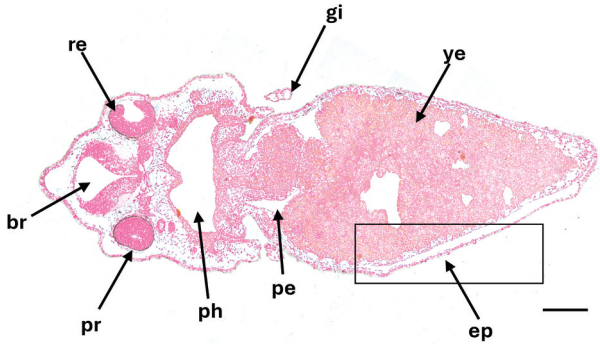

Figure 1. *Pelophylax lessonae*. Section of embryo at Gosner's stage 21 to show the dorsal-lateral region of the epidermis investigated (rectangle). (br) cavity of fore-brain; (ep) epidermis; (gi) gill; (pe) pericardial cavity; (ph) pharynx; (pr) pigmented layer of retina; (re) nervous layer of retina; (ye) yolky endoderm. Mallory's trichrome stain. Scale bar 200 μm.

The basal layer presented basal cells (BC) characterized by flattened ends and a wider central region, in which the euchromatic nucleus was located (Figure 2(a,b)). Mitotic processes were occasionally observed (Figure 2(b), insert).

In the apical layer, four different cell types were observed: ciliated cells, goblet cells, small secretory cells and ionocytes. In all cell types, yolk plates and melanin granules were observed (Figure 2(a,b)).

Ciliated cells (CCs) presented several cilia on the apical surface, wrapped by mucous secretion and an euchromatic nucleus (Figure 2(a)). The whole cytoplasm resulted in PAS positive (Figure 3(a)) and in the basal body region of the apical part, next to the surface, AB 2.5 positivity was observed (Figure 3 C), whereas AB 1 stain resulted negative (Figure 3(f)), suggesting the presence of carboxylated, non-sulphated glycans.

Goblet cells (GCs) were the most abundant cell type and showed apical vesicles secreting mucus. With Toluidine Blue staining (Figure 2(a,b)), the nucleus appeared central and irregular in shape, while the mucus in the vesicles presented different levels of metachromasia, indicating different degrees of acidity. In some cells, it was possible to observe vesicles expelling mucous granules. In the cytoplasmatic portions among secreting vesicles, melanin granules were observed (Figure 2(a, b)). Mucus in the vesicles showed positivity to PAS stain (Figure 3(a,b)) and to AB 2.5 (Figure 2(c,d)), whereas weakly AB 1 stain positivity was observed (Figure 3(e,f)), suggesting the presence of predominantly carboxylated acidic glycans and some sulphated ones. Combined AB-PAS stain resulted in a purplish stain, confirming that all the vesicles secreted acidic glycans (Figure 3(g,h)).

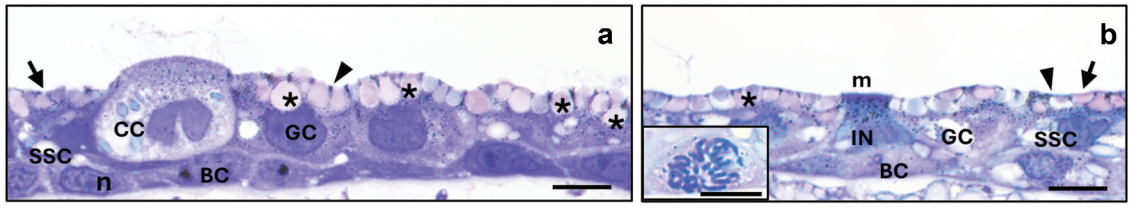

Figure 2. *Pelophylax lessonae*. Sections of embryonic epidermis at Gosner's stage 21. Two layers with five distinct cell types are seen: ciliated cells, with evident long cilia; goblet cells, with apical metachromatic vesicles (asterisk); small secretory cells, with superficial vacuoles (arrow); ionocytes, with apical microvilli (m); basal cells with euchromatic nucleus (n). Goblet and small secretory cells show dark granules (headarrow) among secreting vesicles and/or vacuoles. Insert: basal cell involved in mitotic process.
Abbreviations: BC, basal cell; CC, ciliated cell; GC, goblet cell; SSC, small secretory cell; IN, ionocyte. (a, b): Toluidine Blue. Scale bars 10 μm.

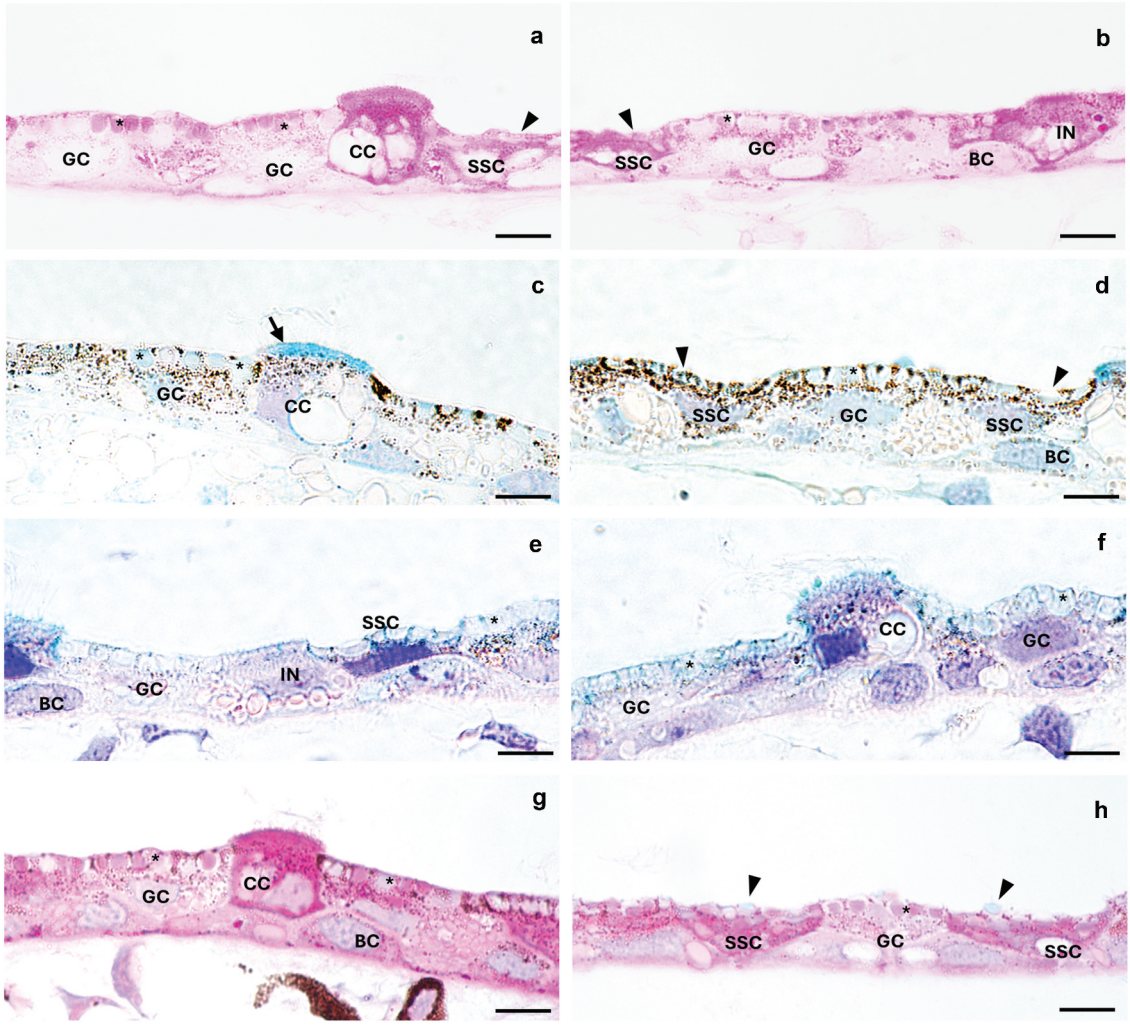

Figure 3. *Pelophylax lessonae*. Sections of embryonic epidermis at Gosner's stage 21. (a-b) section stain with PAS to detect carbohydrates; CCs and INs with PAS positive cytoplasm; GCs present apical positive vesicles (asterisk); SSCs have PAS positive vacuoles (headarrow). Periodic acid-Schiff (PAS). Scale bar 10 µm. (c-d) section stain with AB pH 2.5 to detect acidic glycans. CCs with AB positivity in the basal bodies region (arrow); GCs and SSCs show vesicles (asterisk) and vacuoles (headarrow), respectively. Alcian blue (AB) pH 2.5 – hematoxylin. Scale bar 10 µm. (e-f) section stain with AB pH 1.0 to detect acidic, sulphated glycans. GCs with vesicles weakly positive to AB 1 (asterisk). Alcian blue (AB) pH 1.0 – hematoxylin. Scale bars 10 µm. g-h) section stain with combined AB-PAS. The vesicles of GCs stain in purple (asterisk) indicating the presence of acidic glycans, and some vacuoles of SSCs stain in blue (headarrow), suggesting the prevailing of GAGs. Alcian blue pH 2.5-Periodic acid-Schiff. Scale bars 10 µm.
Abbreviations: BC, basal cell; CC, ciliated cell; GC, goblet cell; SSC, small secretory cell; IN, ionocyte.

Small secretory cells (SSCs) were cup-shaped and characterized by vacuoles on the surface. In respect to GCs, their apical surface presented a deeper concavity, and in the cytoplasm, lower metachromatic material was observed, indicating a less acidic secretion (Figure 2(a,b)). Similar to GCs, abundant melanin granules were observed among the vacuoles (Figure 2(a,b)). The mucous material in the vacuoles of SSCs resulted in PAS (Figure 3(a,b)) and AB 2.5 positive (Figure 3(d)), while AB 1 stained faintly (Figure 3(e)). With AB-PAS, the vacuoles appeared purplish and sometimes completely blue (Figure 3(h)), indicating in some the presence of carboxylated acidic glycans, and in others, the prevailing presence of glycosaminoglycans (GAG), respectively.

In some cases, the vesicles of GCs and the vacuoles of SSCs appeared empty (Figure 3(e,f)).

Ionocytes (INs) had a particularly enlarged cellular shape in the lower portion, narrowing in the apical region, rich in microvilli (Figure 2(b)). Similar to the ciliated cells, the cytoplasm of ionocytes resulted PAS positive (Figure 3(b)). No positivity to the other stains was found for this cell type.

Electron microscopy (SEM; TEM)

The presence of the five cell types previously observed in light microscopy was confirmed by SEM and TEM.

SEM observations allowed to define the distribution of the four cell types of the apical layer of the epithelium (Figure 4). CCs and GCs were scattered throughout the epithelium of the embryo. SSCs were localised predominantly in the dorsolateral and ventral epidermis and less frequently in the caudal epithelium, while INs were exclusively found in the dorsolateral and ventral region. SSCs were often associated with CCs and INs and their vacuoles differed from the vesicles of the GCs for their larger size. INs were smaller and showed a triangular apical surface, with numerous microvilli. Ciliated cells protruded from the surface of the epithelium and showed long cilia on the apical surface (Figure 4).

TEM observations allowed us to observe the details of both the basal and apical layer cells (Figures 5,6).

The basal cells (BCs) were prevailingly electron transparent, with rounded nuclei. Mitotic processes were sometimes observed (Figure 6(f)). No tonofibrils were observed.

GCs showed a low electron-dense cytoplasm, apical vesicles, and a large and irregular-shaped central nucleus (Figure 5(a)). The vesicles were covered by membrane and contained a slightly electron dense secretion, with fine dispersed filaments. It was noted that the secretion was exocytosed via small vesicles (Figure 5(b)). Some vesicles showed a more compact granular secretion, others a granular secretion with a loser network, probably indicating the emptying of those vesicles (Figure 5(b)). Portions of cytoplasm were interdigitated among the secretory vesicles and formed short finger-like projections. Several mitochondria were observed under the apical vesicles (Figure 5(c)).

Small secreting cells showed an electron-dense cytoplasm, a central nucleus, and apical vacuoles containing a uniformly electron-dense material (Figure 5(d)). Vacuoles sometimes exhibited apical membrane disruption, probably as a consequence of exocytosis in the secretion process. The portions of membrane intercalated among the vacuoles presented microvilli protruding from the apical surface. Below the surface, there were vesicles containing probable immature material (Figure 5(e)).

CCs were characterized by numerous cilia on the apical surface (Figure 6(a–c)) and a large nucleus in

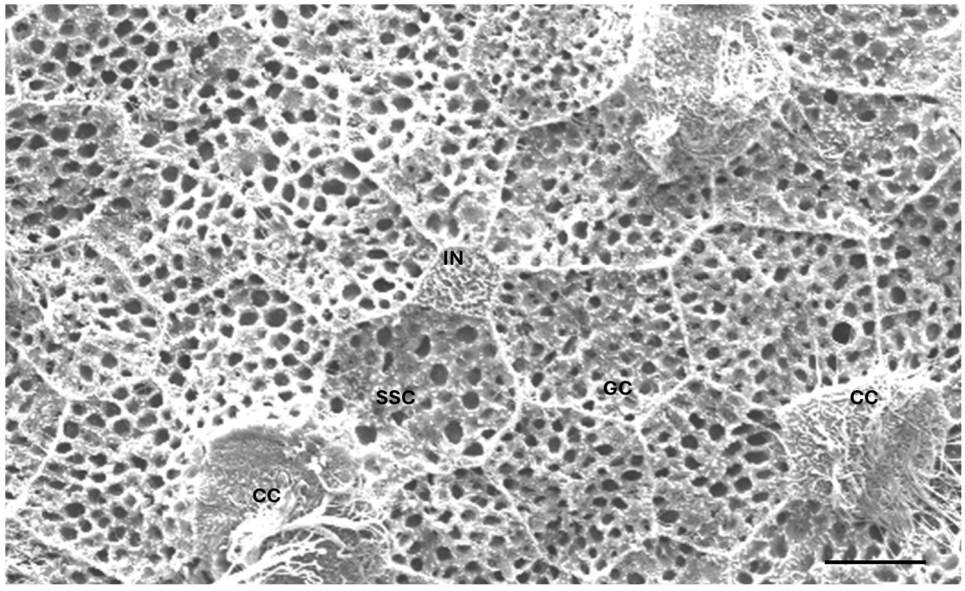

Figure 4. *Pelophylax lessonae*. Embryonic epidermis at Gosner's stage 21. Apical surface view under SEM. In the dorso-lateral and ventral region of embryos four distinct cell types are observed: CCs characterized by the presence of long cilia, GCs with secretory vesicles releasing mucus, SSCs that show large apical vacuoles, INs with numerous microvilli. CCs, SSCs and INs are often clustered. Abbreviations: CC, ciliated cell; GC, goblet cell; SSC, small secretory cell; IN, ionocyte. Scale bar 10 μm.

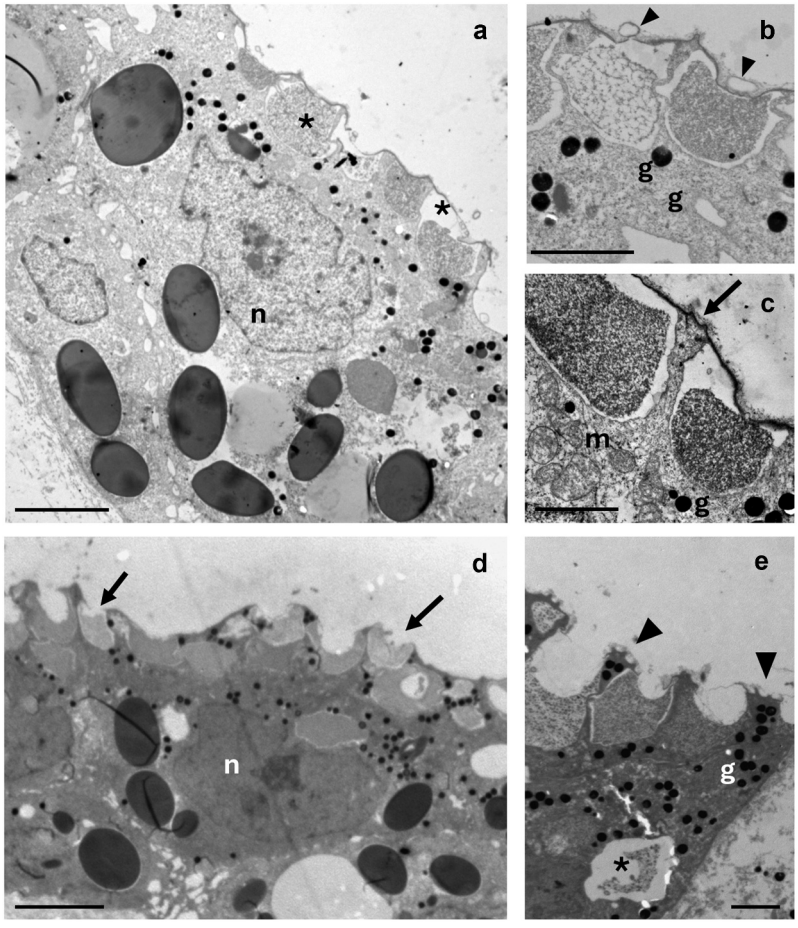

Figure 5. *Pelophylax lessonae*. Sections of embryonic epidermis at Gosner's stage 21 under TEM. (a) GC with low electron-dense cytoplasm, irregular nucleus and mucus-secreting vesicles covered by membrane (asterisk). Scale bar 5 µm (b) detail of GC vesicles with continuous apical membrane, granular secretion and exocytotic vesicles on apical membrane (headarrow). Scale bar 2 µm (c) detail of the cytoplasm of the GC between the secretion vesicles (arrow) and of the mitochondria (m) located just below the vesicles. Scale bar 2 µm (d) SSC with central nucleus, electron-dense cytoplasm and apical vacuoles, with discontinuous membrane (arrow). Scale bar 5 µm (e) detail of vacuoles of SSCs with electron-dense content. Microvilli are present on the apical membrane among vacuoles (head arrow), as well as several melanin granules in the underlying cytoplasm. In the sub-apical portion immature vesicles are often present (asterisk). Scale bar 2 µm.
Abbreviations: GC, goblet cell; SSC, small secretory cell.

their basal portion. Several elongated small vesicles were observed in the sub-apical portion of the cell, exocitosing their secretion (Figure 6(b)). The secretion in these vesicles appeared highly electron-dense, with fine filaments that formed connecting bridges to the cytoplasm of the cell (Figure 6(c)).

Ionocytes appeared with high electron-dense cytoplasm and apical microvilli. There was usually a vacuole inside the cell containing granular material (Figure 6(d)) and small vesicles containing reticular material, just below the apical surface (Figure 6(e)).

No Skein cells were observed.

Discussion

The amphibian embryonic epidermis represents a good model of differentiation, in which the zygote cytoplasm originates a limited number of cell types (e.g. Billett & Gould 1971). This is the case of *P. lessonae* that, at Gosner's stage 21, presents an epidermis with only two layers and five cell types. Thus, we decided to focus on this stage, given that it occurs near hatching and literature data about the embryonic skin of the water frogs in the genus *Pelophylax* are scarce.

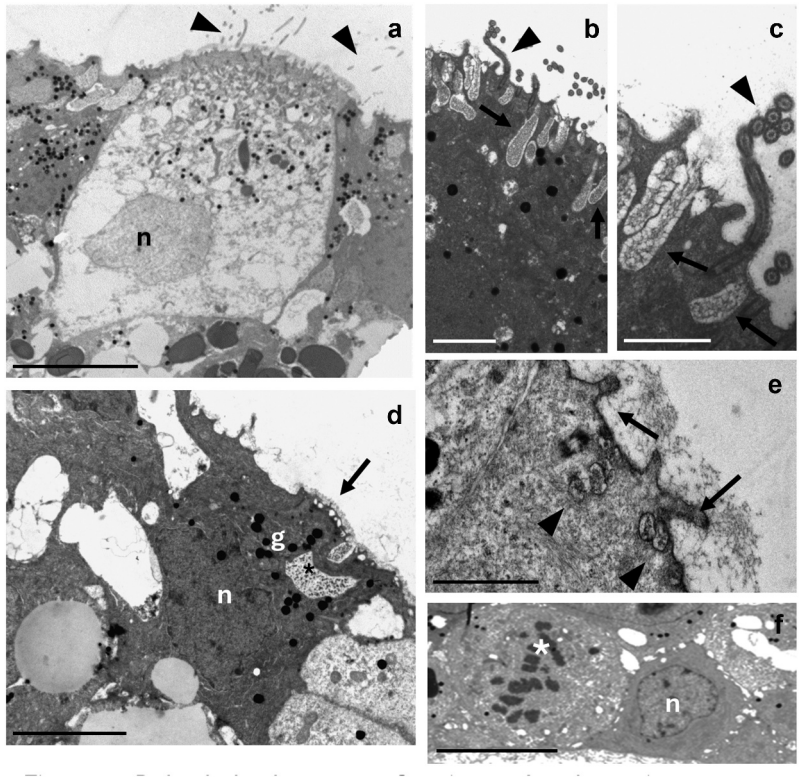

Figure 6. *Pelophylax lessonae*. Sections of embryonic epidermis at Gosner's stage 21 under TEM. (a) CC with central nucleus and apical cilia (head arrow). Scale bar 10 µm; (b,c) detail of the apical portion of a CC in which apical cilia (head arrow) and sub-apical small vesicles (arrow) contain fine electron-dense secretion. Scale bar b 2 µm; scale bar c 1 µm; (d) IN characterized by apical microvilli (arrow) and highly electron dense cytoplasm. A vacuole with granular material is often present in the cell (asterisk). Scale bar 5 µm; (e) detail of apical portion of IN with evident apical microvilli (arrow) and sub-apical small vesicles, containing reticular material (head arrow). Scale bar 1 µm; (f) BC with mitotic figure (asterisk). Scale bar 5 µm.
Abbreviations: BC, basal cell; CC, ciliated cell; IN, ionocyte.

The only observed cells with mitotic activity were the basal cells (BCs) that are reported to keep on dividing during the larval life until metamorphosis (Nishikawa et al. 1990).

Ciliated cells (CCs) showed vesicles under their apical surface. In the upper human respiratory tract, similar cells with a ciliated surface and secretory granules were reported, probably indicating a transitional stage from ciliated to goblet cells (Patel et al. 2011). This has also been hypothesised for the multi-ciliated cells in *Xenopus* embryos, for which trans-differentiation into goblet cells can be an additional mechanism for the removal of such cells from the developing embryo (Nishikawa et al. 1992; Tasca et al. 2021). Furthermore, the consistency of the material in the vesicles of ciliated cells of *P. lessonae* is similar to that observed in *Xenopus laevis* goblet cells at stage 17/23 (according to Nieuwkoop & Faber 1956), with a mass of fibrillar material appearing to be suspended within the vesicle by thin filaments (Billett & Gould 1971), supporting the theory of differentiation towards goblet cells.

Goblet cells (GCs) in *P. lessonae* embryos appear similar to the pavement cells described in *Pelobates cultripes* and *Phyllobates bicolor* tadpoles, storing small dense granules and releasing larger ones (Delfino et al. 2007), as well as to the goblet cells described in *Xenopus tropicalis* in Nieuwkoop & Faber's developmental stage 30 (Dubaissi & Papalopulu 2011), with vesicles arrayed below the apical membrane and a granular content positive to the epidermal lectin, Xeel, also known as intelectin-2 (Nagata 2005, Hayes et al. 2007). The mucus of the goblet cells is similar to that observed in the goblet cells of the swimming larvae of *X. laevis* by Nishikawa et al. (1992), consisting in dense rods with fine filaments. The cited authors detected the presence of chondroitin 6-sulphate by immunoelectron microscopy. Having found AB 2.5 positivity in the secretion of the goblet cells of *P. lessonae*, we can preliminary assume that similar GAGs are present also in this species.

Small secretory cells (SSCs) were probably first described in *X. laevis* differentiated embryonic epidermis, as isolated cells with granules of varying density and unknown function (Billett & Gould 1971), then described as cells with vesicles with a diameter larger than those of goblet cells (Hayes et al. 2007). Recent studies have named and described small secretory cells in *X. tropicalis*, having large vesicles at the apical membrane with dense glycosylated material (Dubaissi et al. 2014). Our glycohistochemical data indicate that in the vesicles of the SSCs of *P. lessonae* embryos there are acidic glycans, mainly carboxylated. Thus, they are probably made by terminal sialic acid and GAGs.

Ionocytes (INs) in frog embryos are a scarcely known cell type. Dubaissi and Papalopulu (2011) described ionocytes in *Xenopus* embryos epithelium as cells that express proton pumps for cellular homeostatic regulation and demonstrated that their absence caused defects in ciliated cells, which resulted in fewer, shorter cilia and impaired ciliary beating. Functionally similar cells have been observed in teleost fish. In fact, the ionocytes of *P. lessonae* embryos are similar to those observed in the larvae of the chum salmon, *Oncorhynchus keta*, and of the Nile tilapia, *Oreochromis niloticus* (Wilson & Laurent 2002; Fridman 2020). Apparently, the vacuole with granular material and the small vesicles with reticular material observed with TEM in the ionocytes of *P. lessonae* embryo epidermis have never been described.

We were not able to observe the Skein cells, probably because at this developmental stage they are not still differentiated and tonofilaments of larval keratin are not yet arranged in the bundles observed at later stages (e.g., Fenoglio et al. 2009).

Conclusions

The present work describes the structure of the epithelium of *P. lessonae* embryos, proposing it as a good experimental model to simulate and/or evaluate the morpho-cellular effects that stress conditions could cause on a mucociliary epithelium. Further histochemical investigations will be conducted for a more in-depth characterization of the mucous secretions. Combined optical and electronic microscopy techniques confirm a promising tool for environmental monitoring, as well as for toxicological studies.

Disclosure statement

No potential conflict of interest was reported by the author(s).

ORCID

D. SEMERARO http://orcid.org/0000-0003-4447-3910
D. MENTINO http://orcid.org/0000-0002-0680-5251
R. ROSSI http://orcid.org/0000-0003-4586-9044
G. SCILLITANI http://orcid.org/0000-0002-5888-7906
M. V. GUGLIELMI http://orcid.org/0000-0003-1296-861X
M. MASTRODONATO http://orcid.org/0000-0002-0799-8032

References

Akat Çömden E, Yenmiş M, Çakır B. 2023. The complex bridge between aquatic and terrestrial life: Skin changes during development of amphibians. Journal of Developmental Biology 11(1):6. DOI: 10.3390/jdb11010006.

Allran JW, Karasov WH. 2001. Effects of atrazine on embryos, larvae, and adults of anuran amphibians. Environmental Toxicology and Chemistry: An International Journal 20 (4):769–775. DOI: 10.1002/etc.5620200411.

Billett FS, Gould RP. 1971. Fine structural changes in the differentiating epidermis of *Xenopus laevis* embryos. Journal of Anatomy 108(Pt 3):465.

Brändli AW. 2004. Prospects for the *Xenopus* embryo model in therapeutics technologies. Chimia 58(10):694–694. DOI: 10.2533/000942904777677443.

Bray D. 2000. Critical point drying of biological specimens for scanning electron microscopy. Supercritical Fluid Methods and Protocols 235–243. DOI: 10.1385/1-59259-030-6:235.

Burggren WW, Warburton S. 2007. Amphibians as animal models for laboratory research in physiology. ILAR journal 48 (3):260–269. DOI: 10.1093/ilar.48.3.260.

Canestrelli D, Nascetti G. 2008. Phylogeography of the pool frog *Rana* (*Pelophylax*) *lessonae* in the Italian peninsula and Sicily: Multiple refugia, glacial expansions and nuclear–mitochondrial discordance. Journal of Biogeography 35 (10):1923–1936. DOI: 10.1111/j.1365-2699.2008.01946.x.

Chammas SM, Carneiro SM, Ferro RS, Antoniazzi MM, Jared C. 2015. Development of integument and cutaneous glands in larval, juvenile and adult toads (*Rhinella granulosa*): A morphological and morphometric study. Acta Zoologica 96 (4):460–477. DOI: 10.1111/azo.12091.

Cuevas A, Patrelle C, Ciavatti F, Gendre T, Sourrouille P, Geniez P, Doniol-Valcroze P, Crochet PA. 2022. A new PCR-RFLP method for the identification of parental and hybridogenetic western European water frogs, including the *Pelophylax perezi-grafi* system. Salamandra 58(3):218–230.

Delfino G, Quagliata S, Giachi F, Malentacchi C. 2007. Kugelzellen in larval anuran epidermis: An ultrastructural study on tadpoles of *Pelobates cultripes* (Pelobatidae) and *Phyllobates bicolor* (Dendrobatidae). Contributions to Zoology 76(4):213–220. DOI: 10.1163/18759866-07604001.

Do Amaral DF, Guerra V, Motta AGC, E Silva DDM, Rocha TL. 2019. Ecotoxicity of nanomaterials in amphibians: A critical review. Science of the Total Environment 686:332–344. DOI: 10.1016/j.scitotenv.2019.05.487.

Dubaissi E, Papalopulu N. 2011. Embryonic frog epidermis: A model for the study of cell-cell interactions in the development of mucociliary disease. Disease Models & Mechanisms 4 (2):179–192. DOI: 10.1242/dmm.006494.

Dubaissi E, Rousseau K, Hughes GW, Ridley C, Grencis RK, Roberts IS, Thornton DJ. 2018. Functional characterization

of the mucus barrier on the *Xenopus tropicalis* skin surface. Proceedings of the National Academy of Sciences 115 (4):726–731. DOI: 10.1073/pnas.1713539115.

Dubaissi E, Rousseau K, Lea R, Soto X, Nardeosingh S, Schweickert A, Amaya E, Thornton DJ, Papalopulu N. 2014. A secretory cell type develops alongside multiciliated cells, ionocytes and goblet cells, and provides a protective, anti-infective function in the frog embryonic mucociliary epidermis. Development 141(7):1514–1525. DOI: 10.1242/dev.102426.

Duellmann WE, Trueb L. 1986. Biology of amphibians. New York, St. Louis: McGraw-Hill.

Dufresnes C, Monod-Broca B, Bellati A, Canestrelli D, Ambu J, Wielstra B, Dubey S, Crochet P-A, Denoël M, Jablonski D. 2024. Piecing the barcoding puzzle of Palearctic water frogs (*Pelophylax*) sheds light on amphibian biogeography and global invasions. Global Change Biology 30(3):e17180. DOI: 10.1111/gcb.17180.

El Mir J, Fedou S, Thézé N, Morice-Picard F, Cario M, Fayyad-Kazan H, Thiébaud P, Rezvani HR. 2023. *Xenopus*: An in vivo model for studying skin response to ultraviolet B irradiation. Development, Growth & Differentiation 65 (4):194–202. DOI: 10.1111/dgd.12848.

Fenoglio C, Grosso A, Boncompagni E, Gandini C, Milanesi G, Barni S. 2009. Exposure to heptachlor: Evaluation of the effects on the larval and adult epidermis of *Rana* kl. *esculenta*. Aquatic Toxicology 91(2):151–160. DOI: 10.1016/j.aquatox.2008.07.005.

Fenoglio C, Grosso A, Boncompagni E, Milanesi G, Gandini C, Barni S. 2006. Morphofunctional evidence of changes in principal and mitochondria-rich cells in the epidermis of the frog *Rana* kl. *esculenta* living in a polluted habitat. Archives of Environmental Contamination and Toxicology 51 (4):690–702. DOI: 10.1007/s00244-005-0245-y.

Fox H. 1974. The epidermis and its degeneration in the larval tail and adult body of *Rana temporaria* and *Xenopus laevis* (Amphibia: Anura). Journal of Zoology 174(2):217–235. DOI: 10.1111/j.1469-7998.1974.tb03153.x.

Fox H. 1986. The skin of amphibia. Epidermis. In: Bereiter-Hahn J, Matoltsy A, Richards K, editors. Biology of the integument. 2: Vertebrates. Berlin: Springer. pp. 78–110.

Fox H. 1988. Riesenzellen, goblet cells, Leydig cells and the large clear cells of *Xenopus*, in the amphibian larval epidermis: Fine structure and a consideration of their homology. Journal of Submicroscopic Cytology and Pathology 20(2):437–451.

Fox H, Hamilton L. 1971. Ultrastructure of diploid and haploid cells of *Xenopus laevis* larvae. Development 26(1):81–98. DOI: 10.1242/dev.26.1.81.

Fridman S. 2020. Ontogeny of the osmoregulatory capacity of teleosts and the role of ionocytes. Frontiers in Marine Science 7:709. DOI: 10.3389/fmars.2020.00709.

Fröhlich J, Dietzmann K, Aurin H. 1978. Zur Histochemie der epidermalen Kugelzelle von Krallenfroschlarven (*Xenopus laevis* Daudin). Acta Histochemica 61(1):155–161. DOI: 10.1016/S0065-1281(78)80059-2.

Giachi F, Tanteri G, Malentacchi C, Delfino G. 2011. Larval epidermis of the red eye tree frog *Agalychnis callidryas* (Anura, Hylidae): Ultrastructural investigation on the Kugelzellen, specialized forms of the constitutive Skein cell line. The Anatomical Record: Advances in Integrative Anatomy and Evolutionary Biology 294(9):1601–1610. DOI: 10.1002/ar.21442.

Gosner KL. 1960. A simplified table for staging anuran embryos and larvae with notes on identification. Herpetologica 16 (3):183–190.

Gristina M, Bertrandino S, Cardone F, Mentino D, Corriero G, Scillitani G. 2017. Skin filament recovery after clipping in *Hippocampus guttulatus*: Behavioural and histological aspects. Aquatic Biology 26:149–157. DOI: 10.3354/ab00680.

Guardabassi A, Campantico E, Grillo A. 1975. Histological observations on the integument of normal and prolactin-treated *Rana esculenta* l. adult males kept at different temperatures. Monitore Zoologico Italiano - Italian Journal of Zoology 9(3–4):163–173.

Guex GD, Hotz H, Uzzell T, Semlitsch RD, Beerli P, Pascolini R. 2001. Developmental disturbances in *Rana esculenta* tadpoles and metamorphs. Zoosystematics and Evolution 77(1):79–86. DOI: 10.1002/mmnz.20010770113.

Guglielmi MV, Mastrodonato M, Semeraro D, Mentino D, Capriello T, La Pietra A, Giarra A, Scillitani G, Ferrandino I. 2024. Aluminum exposure alters the pedal mucous secretions of the chocolate-band snail, *Eobania vermiculata* (Gastropoda: Helicidae). Microscopy Research and Technique 87(7):1453–1466. DOI: 10.1002/jemt.24529.

Harland RM, Grainger RM. 2011. *Xenopus* research: Metamorphosed by genetics and genomics. Trends in Genetics 27(12):507–515. DOI: 10.1016/j.tig.2011.08.003.

Haslam IS, Roubos EW, Mangoni ML, Yoshizato K, Vaudry H, Kloepper JE, Pattwell DM, Maderson PFA, Paus R. 2014. From frog integument to human skin: Dermatological perspectives from frog skin biology. Biological Reviews 89 (3):618–655. DOI: 10.1111/brv.12072.

Hayes JM, Kim SK, Abitua PB, Park TJ, Herrington ER, Kitayama A, Grow MW, Ueno N, Wallingford JB. 2007. Identification of novel ciliogenesis factors using a new in vivo model for mucociliary epithelial development. Developmental Biology 312(1):115–130. DOI: 10.1016/j.ydbio.2007.09.031.

He X, Aker WG, Leszczynski J, Hwang HM. 2014. Using a holistic approach to assess the impact of engineered nanomaterials inducing toxicity in aquatic systems. Journal of Food & Drug Analysis 22(1):128–146. DOI: 10.1016/j.jfda.2014.01.011.

Helmer PJ, Whiteside DP. 2005. Amphibian anatomy and physiology. In: O'Malley B, editor. Clinical anatomy and physiology of exotic animals. Edimburgh: Elsevier Saunders. pp. 3–14.

Johnson MS, Aubee C, Salice CJ, Leigh KB, Liu E, Pott U, Pillard D. 2017. A review of ecological risk assessment methods for amphibians: Comparative assessment of testing methodologies and available data. Integrated Environmental Assessment and Management 13(4):601–613. DOI: 10.1002/ieam.1881.

Leeson CR, Threadgold LT. 1961. The differentiation of the epidermis in *Rana pipiens*. Cells, Tissues, Organs 44(1–2):159–173. DOI: 10.1159/000141717.

Loumbourdis NS. 2005. Hepatotoxic and nephrotoxic effects of cadmium in the frog *Rana ridibunda*. Archives of Toxicology 79(8):434–440. DOI: 10.1007/s00204-005-0652-x.

Masoni A, Garcia-Romeu F. 1979. Moulting in *Rana esculenta*: Development of mitochondria-rich cells, morphological changes of the epithelium and sodium transport. Cell and Tissue Research 197(1):23–38. DOI: 10.1007/BF00233551.

Mastrodonato M, Calamita G, Rossi R, Scillitani G, Liquori GE, Ferri D. 2009. Expression of H^+, K^+-ATPase and glycopattern analysis in the gastric glands of *Rana esculenta*. Journal of Histochemistry & Cytochemistry 57(3):215–225. DOI: 10.1369/jhc.2008.952234.

Mastrodonato M, Mentino D, Lopedota A, Cutrignelli A, Scillitani G. 2017. A histochemical approach to glycan diversity in the urothelium of pig urinary bladder. Microscopy Research and Technique 80(2):239–249. DOI: 10.1002/jemt.22794.

McCoy KA, Peralta AL. 2018. Pesticides could alter amphibian skin microbiomes and the effects of *Batrachochytrium*

dendrobatidis. Frontiers in Microbiology 9:748. DOI: 10.3389/fmicb.2018.00748.

Mentino D, Mastrodonato M, Rossi R, Scillitani G. 2014. Histochemical and structural characterization of egg extracellular matrix in bufonid toads, *Bufo bufo* and *Bufotes balearicus*: Molecular diversity versus morphological uniformity. Microscopy Research and Technique 77(11):910–917. DOI: 10.1002/jemt.22414.

Mentino D, Scillitani G, Marra M, Mastrodonato M. 2017. Seasonal changes in the liver of a non-hibernating population of water frogs, *Pelophylax* kl. *esculentus* (Anura: Ranidae). European Zoological Journal 84(1):525–535. DOI: 10.1080/24750263.2017.1395482.

Nagata S. 2005. Isolation, characterization, and extra-embryonic secretion of the *Xenopus laevis* embryonic epidermal lectin, XEEL. Glycobiology 15(3):281–290. DOI: 10.1093/glycob/cwi010.

Nieuwkoop PD, Faber J. 1956. Normal table of *Xenopus laevis* (Daudin): *A systematical and chronological survey of the development from the fertilized egg till the end of metamorphosis*. Amsterdam: North Holland Publishing Company Ltd.

Nishikawa A, Shimizu-Nishikawa K, Miller L. 1990. Isolation, characterization, and in vitro culture of larval and adult epidermal cells of the frog *Xenopus laevis*. In vitro Cellular & Developmental Biology 26(12):1128–1134. DOI: 10.1007/BF02623689.

Nishikawa S, Hirata J, Sasaki F. 1992. Fate of ciliated epidermal cells during early development of *Xenopus laevis* using whole-mount immunostaining with an antibody against chondroitin 6-sulfate proteoglycan and anti-tubulin: Transdifferentiation or metaplasia of amphibian epidermis. Histochemistry 98(6):355–358. DOI: 10.1007/BF00271070.

Paolucci M, Borriello M, Botte V, Zerani M, Magni AP. 1987. Taxonomic investigations on six populations of the water frog, *Rana esculenta* complex from peninsular Italy and Sicily. Italian Journal of Zoology 54(4):341–346. DOI: 10.1080/11250008709355607.

Patel AC, Brody SL, Stappenbeck TS, Holtzman MJ. 2011. Tracking cell lineage to rediscover (again) the switch from ciliated to mucous cells. American Journal of Respiratory Cell and Molecular Biology 44(3):261–263. DOI: 10.1165/rcmb.2010-0468ED.

Petraccioli A, Maio N, Guarino FM, Scillitani G. 2013. Seasonal variation in glycoconjugates of the pedal glandular system of the rayed Mediterranean limpet, *Patella caerulea* (Gastropoda: Patellidae). Zoology 116(3):186–196. DOI: 10.1016/j.zool.2012.10.006.

Quaranta A, Bellantuono V, Cassano G, Lippe C, Lucia A. 2009. Why amphibians are more sensitive than mammals to xenobiotics. PLOS ONE 4(11):e7699. DOI: 10.1371/journal.pone.0007699.

Quigley IK, Stubbs JL, Kintner C. 2011. Specification of ion transport cells in the *Xenopus larval* skin. Development 138(4):705–714. DOI: 10.1242/dev.055699.

Robinson DH, Heintzelman MB. 1987. Morphology of ventral epidermis of *Rana catesbeiana* during metamorphosis. The Anatomical Record 217(3):305–317. DOI: 10.1002/ar.1092170310.

Rosenberg M, Warburg MR. 1978. Changes in structure of ventral epidermis of *Rana ridibunda* during metamorphosis. Cell and Tissue Research 195(1):111–122. DOI: 10.1007/BF00233680.

Scillitani G, Moramarco AM, Rossi R, Mastrodonato M. 2011. Glycopattern analysis and structure of the egg extra-cellular matrix in the Apennine yellow-bellied toad, *Bombina pachypus* (Anura: Bombinatoridae). Folia Histochemica et Cytobiologica 49(3):06–316. DOI: 10.5603/FHC.2011.0043.

Sim HJ, Kim SH, Myung KJ, Kwon T, Lee HS, Park TJ, Chin W-C. 2018. *Xenopus*: An alternative model system for identifying muco-active agents. PLoS One 13(2):e0193310. DOI: 10.1371/journal.pone.0193310.

Şişman T, Keskin MÇ, Dane H, Adil Ş, Geyikoğlu F, Çolak S, Canpolat E. 2021. Marsh frog (*Pelophylax ridibundus*) as a bioindicator to assess pollution in an agricultural area. Pakistan Journal of Zoology 53(1):337–349. DOI: 10.17582/journal.pjz/20190103130130.

Speybroeck J, Beukema W, Dufresnes C, Fritz U, Jablonski D, Lymberakis P, Martínez-Solano I, Razzetti E, Vamberger M, Vences M, Vörös J, Crochet P-A. 2020. Species list of the European herpetofauna – 2020 update by the taxonomic committee of the societas europaea herpetologica. Amphibia-Reptilia 41(2):139–189. DOI: 10.1163/15685381-bja10010.

Tasca A, Helmstädter M, Brislinger MM, Haas M, Mitchell B, Walentek P. 2021. Notch signaling induces either apoptosis or cell fate change in multiciliated cells during mucociliary tissue remodeling. Developmental Cell 56(4):525–539. DOI: 10.1016/j.devcel.2020.12.005.

Tucci M, Stucci S, Felici C, Cafforio P, Resta L, Rossi R, Silvestris F. 2016. Cilengitide restrains the osteoclast-like bone resorbing activity of myeloma plasma cells. British Journal of Haematology 173(1):59–69. DOI: 10.1111/bjh.13922.

Varga JF, Bui-Marinos MP, Katzenback BA. 2019. Frog skin innate immune defences: Sensing and surviving pathogens. Frontiers in Immunology 9:3128. DOI: 10.3389/fimmu.2018.03128.

Walentek P, Bogusch S, Thumberger T, Vick P, Dubaissi E, Beyer T, Blum M, Blum M, Schweickert A. 2014. A novel serotonin-secreting cell type regulates ciliary motility in the mucociliary epidermis of *Xenopus* tadpoles. Development 141(7):1526–1533. DOI: 10.1242/dev.102343.

Walentek P, Quigley IK. 2017. What we can learn from a tadpole about ciliopathies and airway diseases: Using systems biology in *Xenopus* to study cilia and mucociliary epithelia. Genesis 55(1–2):e23001. DOI: 10.1002/dvg.23001.

Werner ME, Mitchell BJ. 2012. Understanding ciliated epithelia: The power of *Xenopus*. Genesis 50(3):176–185. DOI: 10.1002/dvg.20824.

Wilson JM, Laurent P. 2002. Fish gill morphology: Inside out. The Journal of Experimental Zoology 293(3):192–213. DOI: 10.1002/jez.10124.

Zhelev ZM, Popgeorgiev GS, Angelov MV. 2013. Investigating the changes in the morphological content of the blood of *Pelophylax ridibundus* (Amphibia: Ranidae) as a result of anthropogenic pollution and its use as an environmental bioindicator. Acta Zoologica Bulgarica 65(2):187–196.